THE ASTROPHYSICAL JOURNAL, 381:278–287, 1991 November 1

ABUNDANCES OF Tc AND RELATED ELEMENTS IN STARS OF TYPE M, MS, AND S

ANDREW D. VANTURE,[1] GEORGE WALLERSTEIN,[1,2] AND JEFFERY A. BROWN[1]
Astronomy Department FM-20, University of Washington, Seattle, WA 98195

AND

GRANT BAZAN[3]
Department of Astronomy, University of Illinois, Urbana, IL 61801
Received 1990 October 29; accepted 1991 May 13

ABSTRACT

Abundances of Co, Zr, Nb, and Tc relative to V have been derived for a sample of ten M and MS stars from 0.10 Å pixel^{-1} and 0.04 Å pixel^{-1} Reticon spectra. On a scale with log $N_H = 12.0$ and log $N_V = 4.0$, we find log $N_{Tc} \approx 1.4$ for M stars and 1.0 for MS stars with Tc. It has been suggested by Dominy and Wallerstein that the presence of Tc in M stars which show no enhancements of other *s*-process elements can be explained by a "mini *s*-process". Detailed calculations and the observed abundances of Tc and related elements presented in this study put this interpretation in doubt. Our observations also fail to support the alternative hypothesis suggested by Malaney and Lattanzio that Tc is produced by the photofission of Th and U.

Subject headings: nucleosynthesis — stars: abundances — stars: late-type — stars: long-period variables — stars: semiregular

1. INTRODUCTION

Technetium is the lightest element without any stable isotopes. The half-life of all technetium's isotopes are short by stellar evolutionary standards, so its presence in the atmosphere of a star indicates that it has been produced in the recent past. In our present picture of the nucleosynthesis of many of the elements between the iron peak and ^{209}Bi, heavy elements are created by the capture of neutrons on a time scale longer than the decay time of the unstable isotopes along the neutron capture path (the *s*-process). This scenario was motivated by the detection of Tc I resonance lines in the atmosphere of R And by Merrill (1952), discussed first by Cameron (1954), and subsequently developed by Burbidge et al. (1957). Based upon this picture of nucleosynthesis, the evolution of spectral type on the asymptotic giant branch, AGB, from M → MS → S → SC → C has been explained as episodic helium burning and neutron capture nucleosynthesis in a star's interior followed by the mixing of a portion of the processed material into the envelope of the star (Lambert 1989).

In recent years extensive observations of AGB stars have shown that evolution of the AGB is more complicated and multifaceted than painted in the simple picture given above. In a survey of Tc in 58 stars of spectral types MS and S, Smith & Lambert (1988) find that ~40% of the stars surveyed show enhancements of *s*-processed elements such as Zr, Y, and Ba, but do not show Tc in their spectra. Smith and Lambert interpret these stars as the end products of a mass transfer system similar to the Ba II stars. In an earlier survey of 279 late-type giants and supergiants, Little, Little-Marenin, & Hagen-Bauer (1987, hereafter LLMB) made the surprising discovery that M type Mira variables with periods greater than 300 days tend to show Tc lines though there is no evidence of enhancement of other *s*-process elements. In addition, current models of low-mass AGB stars succeed in producing significant mixing only in low-metallicity stars (Hollowell & Iben 1988; Boothroyd & Sackmann 1988; Lattanzio 1989) while the observations of heavy element enhancements are primarily in disk population stars. Furthermore, recent calculations by Lattanzio & Malaney (1989) and Malaney (1989) suggest that Tc can be producd in detectable amounts in some AGB stars by the photofission of thorium and uranium during the CNO cycle.

In the present study, quantitative abundances of technetium and related elements are obtained for a sample of Mira variables of types M and MS selected from the LLMB survey in order to better understand the nucleosynthetic processes in these stars. When combined with the results of earlier studies (Dominy & Wallerstein 1986 and Wallerstein & Dominy 1988, hereafter DW and WD), the data seem to rule out the theoretical models that produce Tc without creating substantial enhancements of other heavy elements.

2. OBSERVATIONS

The majority of observations in this work were made at the Dominion Astrophysical Observatory, Victoria, British Columbia, with the coudé spectrograph at the 1.2 m telescope using a Reticon detector. Supplemental observations were obtained with the four meter telescope and echelle spectrograph at Cerro Tololo Inter-American Observatory.

Due to the high resolution needed to separate the technetium lines from blends with other weak atomic lines, only bright stars in the LLMB survey were included in our sample. All Mira variables were observed near maximum light. The digital spectra were bias subtracted, flat fielded, and calibrated for wavelength against iron/argon or neon/argon arcs using NOAO's IRAF software package as implemented on the University of Washington's VAX/VMS system.

The spectra of the survey stars observed at DAO cover the wavelength region 3970–4290 Å. The spectra are of two different dispersions: 0.10 Å pixel^{-1} and 0.04 Å pixel^{-1} with an image slicer that yields ~2.3 pixel resolution. The S/N and

[1] Guest Investigator, Dominion Astrophysical Observatory, National Research Council of Canada, Victoria, BC.

[2] Guest Investigator, Cerro Tololo Inter-American Observatory, operated by the Association of Universities for Research in Astronomy under cooperative agreement with the National Science Foundation.

[3] Also Division E, Lawrence Livermore National Laboratory.

TABLE 1

STELLAR PARAMETERS

Star	Spectral Type	Variable Type	$(R-I)_J$	$(V-K)$	T_{eff}[a]	θ_{exc}	Resolution	S/N
R Lyr	M5	SRb	1.91	5.89	3430	2.0	0.10 Å pixel^{-1}	180
TU CVn	M5	SRb	...	6.13[b]	3380	2.0	0.10 Å pixel^{-1}	130
RZ Ari	M6	SRb	2.17[b]	...	3350[c]	2.0	6.0 Å mm^{-1}	photo
R Aql	M7	Mira	...	7.0	3200	2.0	0.04 Å pixel^{-1}	230
T Cep	M6	Mira	...	9.0[b]	3000[d]	2.0	0.10 Å pixel^{-1}	130
o Cet	M5	Mira	1.90	5.87	3430	2.0	0.04 Å pixel^{-1}	130
R Ser	M5	Mira	...	6.71[b]	3500	1.8	0.04 Å pixel^{-1}	230
W Cyg	M5	SRb	2.14	6.39	3330	2.0	0.10 Å pixel^{-1}	130
HR 8062	S4, 1	N.V.	1.56	5.12	3580	1.8	0.10 Å pixel^{-1}	60
RS Cnc.....	S6, 1	SRc	2.33	6.80	3240	2.0	0.04 Å pixel^{-1}	130
χ Cyg.....	S6, 2	Mira	2.68	7.57	3090	1.9	0.04 Å pixel^{-1}	100
o^1 Ori	S3.5, 1	Spectral binary	1.17[c]	...	3700[c]	1.6[c]	2.4 Å mm^{-1}	photo
HR 1105	S3.5, 2	Spectral binary	1.39[c]	...	3700[c]	1.6[c]	2.4 Å mm^{-1}	photo
R And	S3, 5	Mira	2.21[c]	...	3250[c]	2.0[c]	6.0 Å mm^{-1}	photo
T Sgr	S4.5, 8	Mira	...	7.0	3200	1.8	0.2 Å pixel^{-1}	60

[a] Derived from $V-K$ colors using Ridgeway et al. 1980.
[b] Colors from AAVSO and Neugebauer & Leighton 1969.
[c] Values from Wallerstein & Dominy 1988.
[d] Temperature cannot be extrapolated from colors.

dispersion of the spectra for each star are shown in Table 1. The lower resolution spectra include only the 4238 and 4262 Å technetium lines while the range of the high-dispersion spectra was extended to encompass two additional technetium lines at 4049 and 4089 Å. The single echelle spectrum of T Sgr obtained with the CTIO 4 m telescope has a resolution of 0.2 Å.

The continuum in the sample of stars was set after all emission lines known to occur in long-period variables were identified. The measured equivalent widths are given in Table 2 in which the 0.10 Å pixel^{-1} spectra are labeled "low" and the 0.04 Å pixel^{-1} spectra are labeled "high." For some lines only the central depth of the lines was measured and the equivalent width deduced from a central depth—equivalent width curve as defined by the less blended lines.

Of the high-dispersion spectra of the M-type stars with Tc the best-quality spectrum is that of R Ser. The spectrum of R Ser in the region of the Tc I 4238.1 line is shown in Figure 1

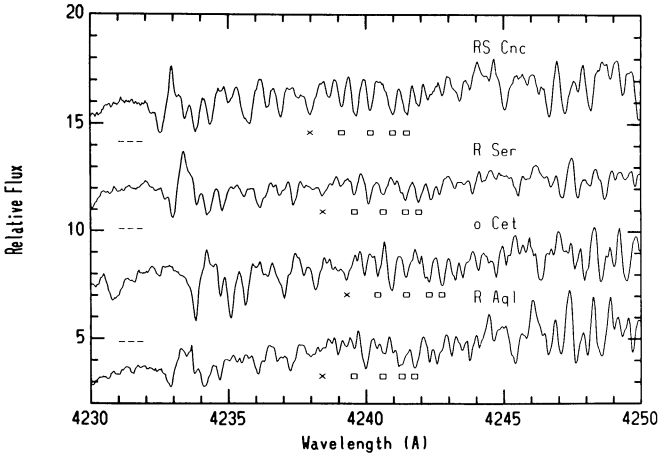

FIG. 1.—Spectra of four stars, RS Cnc an SRc variable of spectral class MS, R Ser an LPV of spectral type M with Tc, *o* Cet another LPV of spectral class M with Tc, and R Aql an LPV without Tc. Crosses indicate the Tc I λ4238 line and the squares indicate the adjacent Zr I lines. The zero point of R Aql's spectrum is at the bottom of the graph, and the zero points of the other spectra are indicated by dashed lines on the right side of the graph.

with the high-dispersion spectra of RS Cnc, *o* Cet, and R Aql. This region includes four Zr I lines. The Fe II λ4233 line commonly seen in emission in long-period variables is prominent in these spectra. The spectral types and variable classifications of each star surveyed are shown in Table 1. Stars observed by DW and WD are included in the table.

3. ANALYSIS AND RESULTS

As has been pointed out by many authors (Hinkle, Hall, & Ridgway 1982; Wallerstein 1985; Smith & Lambert 1986), standard models of cool star atmospheres do not describe realistically the layers of Mira star atmosphere that are responsible for the absorption lines in the blue-violet region. A theoretical discussion emphasizing the magnitude of the shortcomings of static models for the atmospheres of long-period variables is given by Bowen (1989). Therefore, our abundance determinations have proceeded along the same lines as earlier studies of Tc abundances in long-period variables (DW, WD) instead of via the typical spectral synthesis route. As in DW, we have used a standard Schuster-Schwarzschild curve of growth which was calculated for the *Copernicus* project at Princeton University for application to interstellar lines. Also as in DW, the transition probabilities listed in Table 2 have been taken from recent laboratory determinations and the *gf*-values of the Tc I lines are the semi-empirical values calculated by Garstang (1981).

The important input parameters for a curve of growth analysis are the excitation temperature and the microturbulent velocity. The microturbulent velocity was determined using the Zr I lines. Since the majority of Zr is in the form of ^{90}Zr which has a nuclear spin of zero, the velocity given by an analysis of the Zr I lines will not be affected by hyperfine splitting and the velocity can be expected to accurately reflect the Doppler velocity of elements with masses similar to Zr. Typical values of the microturbulent velocity are 2 km s^{-1} (Boesgaard 1970a, b; Smith & Lambert 1985, 1986 (hereafter SL); DW) which is consistent with our analysis of the Zr I lines for our sample of stars. The scatter in the data prevent the determination of v_{micro} to better than 1 km s^{-1}. Therefore, we have adopted a value of $v_{micro} = 2$ km s^{-1} uniformly for our sample

TABLE 2

EQUIVALENT WIDTHS
$[-\log(W/\lambda)]$

			RS Cnc	χ Cyg		R Ser		o Cet	TU CVn	T Cep	HR8062	R Lyr	W Cyg	R Aql	T Sgr
	χ	gf	high	low	high	low	high	high	low	low	low	low	low	low	low
VI															
3990.56	1.85	2.56	...	...	...	...	4.43	...	4.67	4.56	4.41	...	...	...	...
3992.80	1.86	2.51	...	...	...	...	4.53	...	4.59	4.73	4.59	...	4.58	...	...
4113.52	1.22	0.30	...	...	4.46	...	4.30	...	4.19	4.27	4.45	...	4.36	...	...
4123.57	0.27	0.48	...	...	4.21	...	4.23	4.40	4.16	4.15	4.16	4.06	4.08	...	...
4136.09	1.87	0.11	...	...	...	...	...	...	...	...	...	...	4.24	...	...
4136.39	0.29	0.005	4.60	4.34	4.74	4.45	4.84	4.83	4.55	4.33	4.40	4.34	...	...	...
4148.86	0.27	0.003	4.68	...	5.08	4.58	4.98	5.23	4.57	4.67	4.48	...	4.56	...	4.69
4153.33	0.26	0.003	4.59	4.71	4.88	4.56	4.98	4.95	4.49	4.55	4.54	4.49	4.58	...	4.71
4176.79	0.00	0.00065	...	...	4.24	...	4.31	...	...	...	4.23	...	4.24	...	4.47
4182.59	0.28	0.02	4.38	4.46	4.64	4.43	4.81	4.81	4.26	...	4.39	4.24	4.20	...	4.66
4189.84	0.29	0.029	...	...	4.53	...	4.42	4.09	4.38	4.21	4.38	...	...	...	...
4234.52	0.00	0.0065	4.43	...	4.43	4.63	4.68	4.54	4.50	4.11	4.44	4.51	4.56	4.56	...
4259.31	0.02	0.0059	4.54	4.28	4.41	4.43	4.67	4.77	4.27	4.27	4.34	4.29	4.23	4.66	...
CoI															
3978.66	0.51	0.013	...	...	...	4.40	...	...	...	4.40	4.45	...	4.46	...	...
3979.52	0.10	0.0043	4.36	...	...	4.13	4.59	...	4.31	4.26	4.29	...	4.25	...	...
3987.12	0.51	0.0044	4.63	...	...	4.46	4.66	...	4.58	4.43	4.40	...	4.57	...	...
3991.66	0.58	0.0077	4.62	...	...	4.44	4.63	...	4.41	4.46	4.29	...	4.46	...	...
3994.54	0.63	0.0057	4.49	...	...	4.24	4.55	...	4.40	4.28	4.28	...	4.34	...	...
3995.31	0.92	1.4	4.39	...	...	4.52	4.75	...	4.38	4.51	4.34	...	4.33	...	...
4019.30	0.58	0.0025	4.70	...	...	4.40	4.65	...	4.46	4.44	4.51	...	4.41	...	...
4020.90	0.43	0.026	4.35	...	...	4.27	4.50	...	4.27	4.28	4.36	...	4.23	...	...
4066.37	0.92	0.077	...	...	...	4.40	4.62	...	...	4.39	4.36	...	4.29	...	...
4110.54	1.05	0.16	...	...	...	4.50	...	...	4.22	4.36	4.25	4.15	4.19	...	...
4190.71	0.00	0.0028	...	...	...	4.19	...	...	4.16	4.03	4.13	4.17	4.16	...	...
ZrI															
4028.93	0.52	0.19	...	...	...	4.43	4.82	...	4.78	4.75	4.57	...	4.89	...	...
4050.50	0.54	0.20	4.67	...	...	4.54	4.72	4.84	...	4.59	4.40	...	4.46	...	4.79
4061.53	0.52	0.31	4.78	...	...	4.59	4.80	4.88	...	4.63	4.28	...	4.54	...	4.64
4072.70	0.69	2.07	4.58	...	...	4.43	4.66	4.73	4.41	4.44	4.17	...	4.39	...	4.52
4135.68	0.68	0.17	4.59	4.34	4.84	4.55	4.79	4.95	4.50	4.51	4.55	4.54	4.43	...	4.83
4147.37	1.55	0.60	...	...	...	4.70	5.24	5.18	...	...	...	...	...	...	4.71
4171.48	1.35	0.66	...	...	...	4.72	...	...	...	...	...	...	...	...	...
4187.57	1.44	4.6	4.37	4.45	4.50	4.48	4.91	4.67	...	...	...	...	...	...	4.22
4213.87	0.60	0.40	...	...	...	4.59	...	...	4.56	4.22	...	4.55	...	...	4.72
4239.31	0.69	2.30	4.57	4.86	4.62	4.94	4.79	5.16	4.86	4.86	4.64	4.71	4.76	5.21	4.66
4240.35	0.60	0.74	4.65	4.81	4.67	4.71	4.75	5.00	4.57	4.73	4.44	4.49	4.76	4.91	4.70
4241.20	0.62	0.78	4.54	4.58	4.60	4.57	4.70	4.91	4.48	4.24	4.33	4.42	4.40	4.71	4.58
4241.70	0.65	1.40	4.50	4.52	4.55	4.55	4.61	4.75	4.56	4.32	4.47	4.45	4.52	4.54	...
4268.02	0.62	0.30	4.59	4.42	4.48	4.76	4.72	4.88	4.53	4.73	4.33	4.44	...	4.82	4.48
NbI															
4079.71	0.09	2.47	4.43	...	...	4.40	4.64	4.49	...	4.44	4.22	...	4.38	4.34	...
4123.81	0.02	0.89	...	4.41	...	4.45	...	...	4.26	4.45	4.24	4.14	...	...	...
4137.10	0.00	0.37	4.55	4.52	4.80	...	4.81	4.97	...	...	4.38	...	...	4.58	...
4152.60	0.09	0.78	...	4.56	4.97	4.39	4.77	4.82	4.36	...	4.34	4.30	...	...	4.55
4163.65	0.02	0.68	4.60	4.85	4.67	4.54	4.83	4.77	4.52	4.53	4.48	4.49	4.58	...	4.45
4164.64	0.05	0.78	4.48	...	4.72	4.17	4.65	4.55	4.25	4.37	4.27	4.20	4.33	...	4.27
4168.12	0.00	0.47	4.47	4.53	...	4.45	4.67	4.74	4.37	...	4.22	4.22	4.33	...	4.27
4195.09	0.02	0.14	...	4.49	4.44	4.62	...	4.59	...	4.22	4.41	...	4.25	...	...
TcI															
4049.11	0.40	0.87	4.64	...	...	4.59	4.89	4.93	...	...	...	...	...	...	4.58
4088.71	0.46	0.72	4.62	...	...	4.75	5.15	...	...	...	...	...	...	...	4.91
4238.10	0.00	0.38	4.58	4.43	5.08	4.72	4.76	4.96	<5.10	4.48	4.55	<5.10	4.79	<5.39	4.29
4262.27	0.00	0.59	4.48	4.22	4.48	4.53	4.85	4.88	<4.76	4.58	4.11	<4.66	4.36	<5.23	4.22

of stars. As shown in Table 3, even if the turbulent velocity is in error by as much as a factor of 2, the deviation of the derived abundances is still within the given errors (see Table 4). Many of the lines analyzed, in particular the Tc lines, are broadened by substantial hyperfine splitting. If the hyperfine splitting (hfs) is not taken into account, the errors introduced in the derived abundances can be large. For these lines the hfs patterns are approximated by Gaussian distribution of components which are converted to a velocity equivalent. Then the quadratic sum of the turbulent velocity and hyperfine velocity are used as the velocity parameter in the curve of growth analysis. Approximating the hfs of the Tc lines by a Gaussian velocity profile

TABLE 3

SENSITIVITY OF ABUNDANCE TO V_{micro} AND θ_{exc} FOR R SER

	θ_{exc}/v		
ABUNDANCE	1.6/2	1.8/2	1.8/4
V	4.0	4.0	4.0
Zr.....	2.9	3.0	2.95
Nb.....	1.7	1.6	1.7
Tc.....	1.7	1.7	2.0
Coo.....	5.0	5.0	5.1

may lead to inaccuracies in the derived abundances because the distribution of hyperfine components is often boxy rather than a smoothly varying distribution of components. In the extreme case in which the velocity equivalent of the hyperfine pattern is taken to be the full velocity width of the line profile, the errors introduced can be as large as 0.6 dex for the strongest lines [$\log(W/\lambda) = -4.55$]. However, because the contributions of individual hyperfine components is not evenly distributed, this is certainly an overestimate of the errors introduced by this approximation. Additionally, most of the Tc lines used have equivalent widths 0.1 dex smaller than this. The error introduced in the derived abundances from the weaker lines would be at most 0.3 dex. These errors are further ameliorated when the abundances derived from individual lines are averaged together.

Due to the limited spectral coverage necessitated by the need for high resolution and the limited range of excitation potentials of the lines measured, θ_{exc} could not be obtained directly in the manner typical of a classical curve of growth analysis. Instead, the value of θ_{exc} is based upon the $(R-I)_J$ and $(V-K)$ colors of the sample stars. The effective temperatures are derived using the scale of Ridgway et al. (1980). These data are shown in Table 1 along with other basic information pertaining to the sample of stars. As shown in Table 3, the abundances derived by our curve of growth analysis are relatively insensitive to the θ_{exc} parameter.

In order to derive absolute abundances from the relative abundances derived in the curve of growth analysis, it is necessary to chose an element to use as a "zero point." We have chosen vanadium for the zero point because it has many low-excitation lines in the region of interest and the abundance is not expected to be altered by the nucleosynthetic processes which could produce Tc. Therefore, for all stars, the logarithmic abundance of V has been set at its solar value of 4.0 (Anders & Grevesse 1989). The abundances derived using this scale are shown in Table 4. The abundances shown in Table 4 were derived from high-dispersion spectra for the stars RS Cnc, χ Cyg, R Ser, o Cet and R Aql. All other abundances are derived from the lower dispersion spectra. Zirconium is used as the zero point in R Lyr, W Cyg, and R Aql because the number of weak vanadium lines was too small to accurately fix the zero point of the abundance scale. Since those stars are of type M, we have set the Zr to its solar value ($\log N_{Zr} = 2.6$).

Errors in the curve of growth analysis of long-period variables are difficult to quantify and propagate Setting the continuum, blending due to weak lines, and errors in the values of the transition probabilities are some of the effects which introduce errors in the analysis. These errors are mitigated in our analysis by deriving an abundance for each line falling near the linear part of the curve of growth ($\log W/\lambda < -4.55$ for $v = 2$ km s^{-1} and somewhat higher for larger velocities), then averaging the abundances derived from each line to obtain an overall abundance for each element. An error can be assigned

TABLE 4

LOG Tc, Zr, Nb, AND Co ABUNDANCES RELATIVE TO V[a]

Star	Zr	Nb	Tc	Co
Sun	2.6	1.4	...	4.9
M Stars without Tc				
R Lyr	2.6[b]	1.15	< -0.35	...
TU CVn	2.55 ± 0.25	1.4 ± 0.2	<0.1	4.7 ± 0.2
RZ Ari[c]	2.3 ± 0.2	1.0 ± 0.4	< -0.1	...
R Aql	2.6[b]	...	<0.9	...
Average	2.4	1.2	<0.1	...
M Stars with Tc				
T Cep	2.3 ± 0.3	1.05 ± 0.4	1.3 ± 0.4	4.35 ± 0.25
o Cet	2.9 ± 0.1	1.6 ± 0.1	1.4 ± 0.1	4.3 ± 0.34
R Ser	3.0 ± 0.1	1.6 ± 0.1	1.7 ± 0.2	5.0 ± 0.3
W Cyg	2.6[b] ± 0.4	1.4 ± 0.2	1.35 ± 0.4	5.45 ± 0.4
Average	2.7	1.4	1.4	4.6
MS Stars with Tc				
HR 8062	2.4 ± 0.5	...	0.9	4.4 ± 0.3
RS Cnc	2.3 ± 0.2	1.1 ± 0.2	1.3 ± 0.3	4.8 ± 0.2
χ Cyg	3.15 ± 0.2	1.5 ± 0.2	1.4	4.6 ± 0.45
o^1 Ori[c]	2.8 ± 0.2	1.1 ± 0.2	0.5 ± 0.1	4.4 ± 0.3
Average	2.7	1.2	1.0	4.6
S Stars without Tc				
HR 1105[c]	3.4 ± 0.2	2.2 ± 0.2	<0.5	4.05 ± 0.6
S Stars with Tc				
R And[c]	3.3 ± 0.2	2.1 ± 0.4	1.2 ± 0.2	...
T Sgr	2.9 ± 0.2	2.1 ± 0.4	1.85 ± 0.2	...

[a] V set at 4.0.
[b] Value set at solar abundance.
[c] Zr, Tc, and Nb abundances from Wallerstein & Dominy 1988.

as the standard deviation of these measurements. These errors are given in Table 4. Other errors may be introduced by applying the Schuster-Schwarzschild curve of growth which is calculated for an LTE, plane-parallel atmosphere to the intrinsically complicated atmospheric structure of a red giant star. These effects have been minimized in this study by using elements with similar ionization potentials (6.7 → 7.6 eV) and lines with a limited range of excitation potentials (0.0–1.8 eV). Thus, one expects line formation to be confined to a relatively thin layer of the atmosphere in which the Schuster-Schwarzschild approximations will be appropriate.

Some insight into the errors inherent in this analysis may be gained by a comparison of the abundances derived from the high- and low-resolution spectra. Two stars included in this investigation were studied at both the high and low resolutions—R Ser and χ Cyg. In the case of R Ser, the high-resolution spectra resulted in a Zr abundance 0.2 dex larger, a Nb abundance 0.15 dex larger, and a Tc abundance 0.6 dex larger than in the lower dispersion spectrum. For χ Cyg, the higher resolution spectrum gives a Zr abundance 0.1 dex larger, a Nb abundance 0.3 dex larger, and a Tc abundance 0.3 dex smaller. The higher dispersion spectra will give more reliable results in general because the effects of blending should be reduced and more lines of all elements were measured and analyzed. In particular, the higher dispersion spectra allow us to use four lines of Tc rather than the two which are accesible with the lower dispersion. In any case, the differences are within the expected uncertainties in the analysis of spectra of cool stars with substantial blending.

Improved model atmospheres for cool M giant stars have become available recently (Brown et al. 1989). Attempts were made to synthesize the spectra of R Ser in the region of the 4238 Å Tc I line using a subset of these models with $T_{\rm eff}$ = 3200, 3400, 3600, $\log(g) = 0.0$ and 1.0, and solar composition. As with the attempts of previous investigators (DW), it was found that the line strengths in the synthesis were much too strong, so this approach was abandoned. The inapplicability of model atmospheres to the blue-violet lines of Mira stars is almost certainly due to the layered structure of their atmospheres (Hinkle, Hall, & Ridgway 1982; Wallerstein 1985).

A comparison of the abundance of Nb as derived from our 1988 spectrum of *o* Ceti and the abundance of Nb reported by Dominy & Wallerstein (1986) from a 1979 spectrum reveals a drastic change in the relative abundances of Nb and Zr. In 1988 Zr/Nb was 1.3 dex as compared with 2.5 dex in 1979! Upon comparison of the equivalent widths published by Dominy and Wallerstein and the equivalent widths measured in this study, we find large differences between the two observations. While the mean equivalent width of the Zr lines was 0.17 dex lower in 1988 than in 1979 (and lines of V and Tc changed similarly), lines of Nb were 0.14 dex higher. (A parallel analysis of RS Cnc shows systematic shifts in the equivalents widths of Nb and Zr also. However, the shifts, are the same magnitude and in the same direction for RS Cnc). Since no other star on our program has ever shown the low Nb abundance of *o* Ceti in 1979, we can only surmise that Nb was substantially ionized when those observations were obtained despite the fact the phases of the 1988 and 1979 observations are identical and the ionization potential of Nb, 6.77 eV, lies between that of V, 6.74 eV, and that of Zr, 6.95 eV. A difference in ionization ratios among these elements from star to star and from time to time for the same star can only be due to large departures from local thermodynamic equilibrium (LTE).

Departures from LTE would not be surprising in a long period variable but the cause of these departures is obscure in this case. It is natural to suspect non–LTE ionization by scattered Lyα photons whose local intensity should vary with phase and from cycle to cycle as do the Balmer emission lines. If the photoionization crosssection by 10.15 eV photons for Nb were substantially larger than for nearby elements we could pin the blame on Lyα. However, calculations by A. L. Merts and J. Abdallah of the Los Alamos National Laboratory for Nb, Tc, and Co (see below for the importance of cobalt) show that the cross sections for photoionization from the ground and first excited states are almost the same for Nb and Tc while for Co they are smaller. Hence, departures from LTE by Lyα photoionization cannot explain the low apparent Nb abundance in 1979.

4. DISCUSSION

4.1. *Comparison with Other Recent Surveys*

Prior to discussing the abundances obtained for our sample of stars, it is worth reviewing our high-resolution spectra in the context of the LLMB survey of Tc. The stars in the LLMB study are classified in several categories depending upon the confidence with which Tc is detected. Our survey stars fall into three of the five categories defined by LLMB: "yes" which indicates the presence of the three resonant Tc I lines 4238, 4262, and 4297 Å; "probable" based upon the presence of the 4297 Å line in a blend with a Sm I and Ce II line; and "doubtful" which indicates that the Tc I resonance lines are too weak to identify with any certainty. Table 5 lists the LLMB classification, our classification, and the lines identified in each star of our survey. We find that all stars in our survey which fall into the "yes" category of LLMB survey show Tc. Of our survey stars which fall into the "probable" category, W Cyg and o^1 Ori show Tc while TU CVn does not. TU CVn, whose period is 50 days, does not show Tc although listed as "probable" by LLMB. This result is not surprising since it is the only SRb M giant in their survey with a period of less than 100 days to possibly show Tc. Therefore, reclassification of this star puts it in general agreement with the results of the LLMB survey. Last, no survey star classified as "doubtful" by LLMB shows Tc.

Several other studies have been conducted in which Tc abundances in late-type stars have been derived. In recent work, Smith (1988), SL, and Kipper & Kipper (1984) have derived Tc abundances for samples of MS and S stars. Comparison of present results with those studies shows that there are large disagreements among the studies. However, it should be pointed out that this study has several advantages over the previous studies. First, for many of our stars we have higher resolution spectra than in either the SL or Kipper study (0.2 Å for SL and ~0.3 Å for Kipper vs. 0.10 Å for this study). This should be significant in reducing the uncertainties introduced by blending of other lines with the Tc lines which is always a problem in cool star analyses. Second, we have derived abundances from four lines of Tc in many cases while SL and Kipper use one and two lines, respectively. Furthermore, these four lines all yield Tc abundances which agree. Last, the choice of the excitation and ionization potentials of the lines and elements we have used as comparisons for Tc should place tighter constraints on the derived abundances in the kind of parameterized study which is conducted when curve of growth or spectral synthesis analyses are used: the more restricted

TABLE 5

LINE IDENTIFICATIONS

STAR	Tc		LINES IDENTIFIED			
	LLMB	This Study	4049	4088	4238	4262
R Lyr	doubtful	no	...	...	...	...
TU CVn	probable	no	...	...	...	...
RZ Ari	...	no	...	...	...	...
R Aql	doubtful	no	...	...	...	...
T Cep	yes	yes	...	...	X	X
o Cet	yes	yes	X	...	X	X
R Ser	yes	yes	X	X	X	X
W Cyg	probable	yes	...	...	X	X
HR8062	yes	yes	...	...	X	X
RS Cnc	yes	yes	X	X	X	X
χ Cyg	yes	yes	...	...	X	X
o^1 Ori	probable	yes	X	X	X	X
HR1105	doubtful	no	...	...	...	...
R And	yes	yes	X	X	X	X
T Sgr	yes	yes	X	X	X	X

selection of lines should act to minimize the systematic effects of an incomplete or incorrect model atmosphere. A more detailed comparison of our results with those of the Texas and Tartu groups is given in Appendix A.

4.2. *Implications for Nucleosynthesis*

The quantitative abundances of Tc and elements close to it in the periodic table give some insight into the nucleosynthetic processes occurring as the stars evolve in spectral type from M to S. In particular, the appearance of Tc in the spectrum of a star is generally heralded to be the hallmark of the *s*-process. Of particular interest in the context of the *s*-process are the abundances of Zr and Tc. Due to their vastly different neutron capture cross sections, the relative abundances of these elements will be affected differently by different levels of neutron irradiation. The abundances given in Table 4 make it apparent that in all stars in our survey showing Tc, the abundance of Tc is roughly the same, whereas the Zr is enhanced in the S stars as expected, but hardly enhanced in the MS and M stars with Tc as compared to the normal M stars.

The standard differential equation used to describe the *s*-process capture chain (omitting the delays caused by slow β-decays) is

$$dN_A/d\tau = \sigma_{A-1} N_{A-1} - \sigma_A N_A , \quad (1)$$

where σ is the neutron capture cross section and τ, the integrated neutron exposure, is defined by the integral

$$\tau = v_T \int_0^\infty n_n(t) dt \quad (2)$$

in which n_n is the neutron density and v_T is the thermal velocity of the neutrons and the units of τ are inverse millibarns (mb^{-1}). When the *s*-process has reached an equilibrium $dN_A/d\tau = 0$ and the condition $\sigma_{A-1} N_{A-1} = \sigma_A N_A$ holds for adjacent isotopes. This implies that the ratio of abundances for any two nonmagic nuclei close to one another on the *s*-process chain should be given by

$$N_A/N_B = \sigma_B/\sigma_A . \quad (3)$$

However, ^{90}Zr is a neutron magic nucleus, so calculating the Tc/Zr ratio requires a much more detailed, equilibrium calculation of the *s*-process. Such calculations have been conducted and are summarized by Cowley & Downs (1980). These calculations indicate that the Tc/Zr ratio should fall in the range $-2.6 \leq \log (N_{Tc}/N_{Zr}) \leq -2.0$ when the *s*-process has reached equilibrium. From the abundances given Table 4, it is seen that for the prototypical S star, R And, $\log (N_{Tc}/N_{Zr}) = -2.1$ indicating that the abundances in the atmosphere of R And reflect an equilibrium distribution of *s*-process elements. The ratio of Tc/Zr in T Sgr does not fall into the expected range of values; however, the Zr abundance derived is rather smaller than expected for an S star and the Tc abundance is much larger than the Tc abundances derived for other stars in this study. This may be a reflection of the fact that the zero volt lines of Tc I, 4238 and 4262 Å, are much too strong to be used to derive abundances so the abundances are derived from the 0.6 eV lines 4049 and 4088 Å. There is a further caveat that may apply to T Sgr. It shows the strongest Li I resonance line of any S star yet surveyed (Boesgaard 1970b; Ake 1977). In this respect it is similar to the SC stars (Kipper & Wallerstein 1990) whose atmospheres have very low boundary temperatures. Hence all strong zero volt lines of neutral metals may be enhanced and may yield spuriously high abundances.

However, the appearance of Tc without a simultaneous enhancement of other heavy elements does not occur in the standard scenarios of the *s*-process. Dominy & Wallerstein (1986) have suggested that a nonequilibrium "mini *s*-process" in which each seed nucleus captures one and only one neutron could be responsible for the presence of Tc in M stars. Such a process would create Tc via the reactions ^{98}Mo(n, γ) ^{99}Mo($\beta^- \nu$)^{99}Tc and ^{96}Ru(n, γ)^{97}Ru($\beta^+ \nu$)^{97}Tc while leaving the abundance of Zr almost unchanged. DW calculate abundances of Tc and related elements by solving the standard differential equations under the assumption of a single δ-function impulse of neutrons.[4] This calculation is quasi-static in nature and does not take into account cases in which β decays compete with neutron captures. In addition, it is a poor approximation because the neutron capture cross section of ^{99}Tc is so large that ^{99}Tc begins to be depleted by neutron capture before its production from ^{98}Mo is complete. A more thorough nonequilibrium calculation has been performed for

[4] There is a sign error in eq. (2) of DW. The equation should read

$$^AX = {}^{A-1}X[1 - \exp(-\tau\langle\sigma v\rangle_{A-1}] + {}^AX_0 \exp(-\tau\langle\sigma v\rangle_A)$$

TABLE 6

CALCULATED *s*-PROCESS ABUNDANCES

ISOTOPE	INITIAL ABUNDANCE (log N)	$\langle\sigma v\rangle$ (mb)	FINAL ABUNDANCES[a] DW ($\tau = 0.01$)	Exact Mini *s*-Process $\tau = 0.002$	$\tau = 0.01$	$\tau = 0.03$
^{58}Ni	6.1	38	5.9	6.05	5.9	5.4
^{59}Ni	...	104	5.6	5.0	5.5	5.3
^{60}Ni	5.7	31	5.5	5.7	5.7	6.0
^{61}Ni	4.3	82	5.15	4.71	5.1	5.4
^{62}Ni	4.8	36	4.7	4.8	5.1	5.6
^{64}Ni	4.2	10	4.3	4.2	4.4	4.9
ΣNi	6.3	...	6.2	6.3	6.3	6.3
^{59}Co	4.9	38	4.9	4.9	5.2	6.0
^{89}Y	2.2	21	2.3	2.2	2.3	2.4
^{90}Zr	2.3	16	2.3	2.3	2.3	2.3
^{91}Zr	1.6	60	1.7	1.7	1.8	1.8
^{92}Zr	1.6	50	1.75	1.9	1.9	2.0
^{93}Zr	...	95	1.4	0.8	1.3	1.5
^{94}Zr	1.8	33	1.65	1.8	1.8	1.9
^{96}Zr	1.0	40	0.8	1.1	1.0	0.9
ΣZr	2.6	...	2.6	2.6	2.65	2.7
^{93}Nb	1.4	271	0.9	1.15	0.4	−0.5
^{92}Mo	1.1	70	0.8	1.1	0.7	−1.1
^{94}Mo	0.9	104	1.4	1.3	1.2	0.4
^{95}Mo	1.1	374	0.7	1.1	1.1	0.9
^{96}Mo	1.1	103	1.2	1.3	1.5	1.4
^{97}Mo	0.9	384	0.9	1.0	1.1	1.0
^{98}Mo	1.2	102	1.2	1.4	1.5	1.6
^{100}Mo	0.9	97	0.5	0.8	0.4	−0.7
ΣMo	1.9	...	1.9	2.0	2.0	1.9
^{96}Ru	0.6	270	−0.6	...	...	...
^{97}Tc	...	412	0.6	0.0	−0.8	−3.8
^{98}Tc	...	1157	...	−0.8	−1.6	−4.5
^{99}Tc	...	732	1.1	0.4	0.6	0.7
ΣTc	...	...	1.2	0.6	0.6	0.7

[a] The long-lived isotopes, ^{59}Ni, ^{93}Zr, ^{97}Tc, ^{98}Tc, and ^{99}Tc have not been allowed to decay.

this study. Quantitatively, the abundances resulting from this more exact "mini *s*-process" are determined by solving the coupled differential equations,

$$\frac{dY(Z, A)}{dt} = \lambda_{\beta+}(Z + 1, A)Y(Z + 1, A) + \lambda_{\beta}(Z - 1, A)Y(Z - 1, A) + n_n\langle\sigma v(Z, A - 1)\rangle Y(Z, A - 1) - [\lambda_{\beta+}(Z, A) + \lambda_{\beta}(Z, A) + n_n\langle\sigma v(Z, A)\rangle]Y(Z, A) , \quad (4)$$

where $Y(Z, A)$ is the abundance of an isotope of charge Z and mass A; $\lambda_{\beta+}$ and λ_{β} are the beta decay rates; n_n is the neutron density, and $\langle\sigma v\rangle$ is the mean neutron capture cross section weighted by velocity.

The abundances of Tc and related elements as a function of τ are solved using equation 4 with a network of 613 nuclei from ^{12}C to ^{210}Po, a neutron density of 1×10^8 cm^{-3} and a temperature of 3×10^8 K. Long-lived isotopes such as ^{99}Tc have not been allowed to decay. The temperature dependent beta and positron decay rates are adopted from Takahashi & Yokoi (1987) while neutron cross sections have been taken from Bao & Käppeler (1987) with additions from Ratynski & Käppeler (1988) and Beer, Käppeler, & Arcoragi (1989). Temperature dependences of the neutron capture rates due to nuclear state population effects are estimated via results presented in Holmes et al. (1976) and Woosley et al. (1978). The abundances calculated using the exact "mini *s*-process" scheme for a τ of 0.002, 0.01, and 0.03 are shown in Table 6 along with abundances calculated using the DW scheme ($\tau = 0.01$) for comparison. Upon comparison with Table 4, it can be seen that all program stars which contain Tc have abundances at the level of log $(N_{\rm Tc}) \approx 1.2$ while the model produces a maximum value of log $(N_{\rm Tc}) \approx 0.7$. Clearly this nonequilibrium model does not produce adequate Tc abundances to account for the observations of M and MS stars in this study. This is due in part to the fact that the condition that a single neutron capture per nuclei of Tc cannot be achieved in reality. Even at very low neutron exposures the exceptionally large cross-sections of the Tc isotopes make multiple neutron captures common.

In addition to the above calculations a larger volume in parameter space has been explored by calculating the abundances of Tc, Zr, and Nb at several values of neutron density and temperature. The results of these calculations are shown for a representative temperature, 2×10^8 K, in Figures 2 and 3.[5] The ratio of Tc to Nb and Zr are shown for various admix-

[5] The derived abundance ratios among the elements considered change only slightly with temperature in the range of 2–3 $\times 10^8$ K.

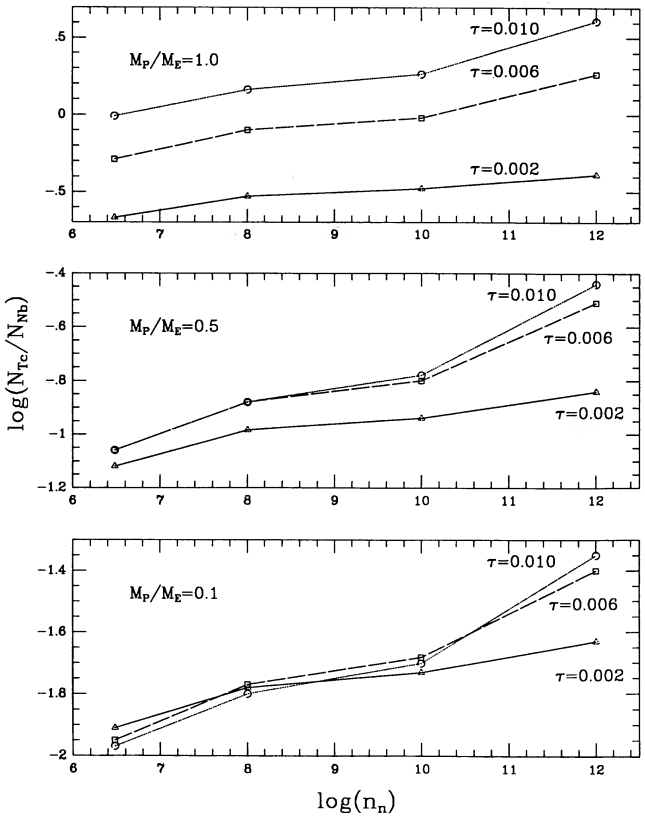

FIG. 2.—Logarithmic abundance ratio of Tc/Nb as a function of the neutron density n_n, for several values of the integrated neutron flux, τ, and admixtures of processed material, M_P, and envelope material, M_E for $T = 2 \times 10^8$ K.

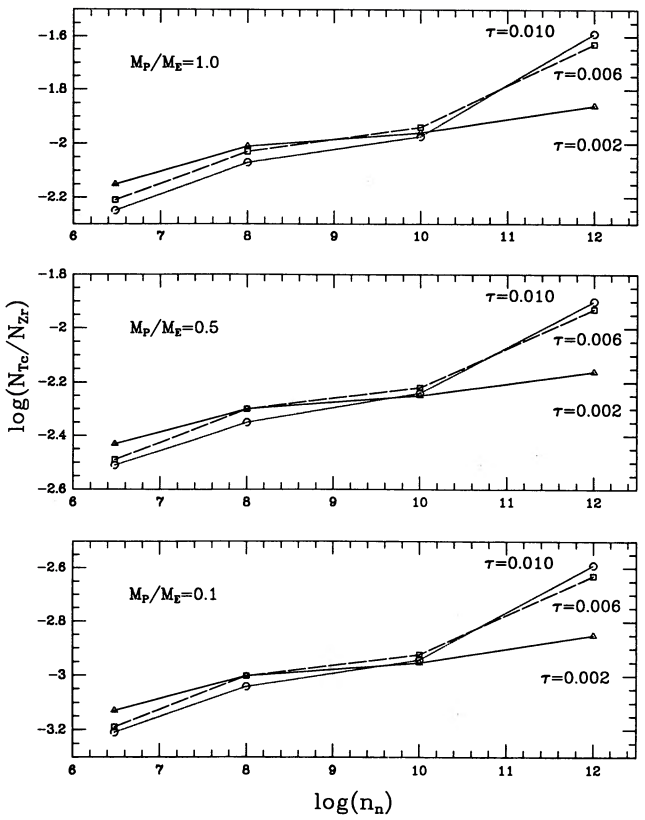

FIG. 3.—Logarithmic abundance ratio of Tc/Zr as a function of the neutron density, n_n, for several values of the integrated neutron flux, τ, and admixtures of processed material, M_P, and envelope material, M_E for $T = 2 \times 10^8$ K.

tures of processed material, M_P, with envelope material, M_E. The mixing ratios are calculated in the following fashion. The ratio $M_P/M_E = 1.0$ indicates that the envelope material of the star consists entirely of processed material while the ratio $M_P/M_E = 0.1$ indicates the envelope material of the star consists of 10% processed material and 90% unprocessed material which is assumed to have solar abundance ratios.

From Figures 2 and 3, it is apparent that the Tc/Zr and Tc/Nb abundance ratios are effected differently by differing admixtures of unprocessed material. In the "mini *s*-process," the Zr abundance in the processed material is unaffected by the low neutron exposures, so the overall abundance of Zr remains unchanged. Thus, when processed and unprocessed material are mixed, the Zr abundance will not change, but the Tc abundance will be diluted. Therefore, the net effect of mixing processed and unprocessed material on the Tc/Zr ratio is to simply scale the ratio with degree of dilution. The Tc/Nb ratio, on the other hand, is a bit more complicated. Niobium consists of only one stable isotope, ^{93}Nb, created by the decay of the unstable isotope ^{93}Zr which has a half-life of 1.5×10^6 yr. Since the mixing time scale in the star is considerably shorter than a million years, ^{93}Zr is not allowed to decay to Nb in our calculations. Therefore, the effect of the "mini *s*-process" is to destroy Nb in the processed material while at the same time creating Tc. Thus, when the processed material is mixed with unprocessed material which contains Nb but no Tc, the result is to increase the Nb abundance while decreasing the Tc abundance. Therefore, the Tc/Nb ratio is particularly sensitive to the mixing ratio and is a more accurate indicator of the amount of mixing in the star's atmosphere.

The observed abundances shown in Table 4 show that the M stars surveyed have typical values of $\log (N_{Tc}/N_{Nb}) \approx 0.0$ and $\log (N_{Tc}/N_{Zr}) \approx -1.3$ and the MS stars have typical values of these ratios of $\log (N_{Tc}/N_{Nb}) \approx -0.2$ and $\log (N_{Tc}/N_{Zr}) \approx -1.7$. Within the given errors, these ratios are the same for both M and MS stars. Upon inspection of Figure 3, it can be seen that the only scenario which will account for the Tc/Zr ratios in M and MS stars is one in which $M_P/M_E \approx 1.0$, $n_n \geq 10^{10}$ cm^{-3}, and any value of τ from 0.006 to 0.01 is permitted. As stated above, the Tc/Nb ratio places much more stringent constraints on the mixing scenario. Upon inspection of Figure 2, it is apparent that the best fit for the Tc/Nb ratio in M and MS stars can be achieved when $\tau \approx 0.006$–0.010 mb^{-1} and $n_n \geq 10^7$ but $n_n \leq 10^{10}$ (for $\tau = 0.01$) for $M_P/M_E \approx 1.0$. However, lower values of the neutron density at higher values of τ cannot be excluded. The limits placed on the neutron density by the Tc/Nb ratio are consistent with the values of n_n found from Zr isotope ratios in other cool, evolved stars (Zook 1985; Smith 1988). As Figures 2 and 3 show, any substantial dilution of processed material with unprocessed envelope material makes a fit to the observed values of Tc/Nb and Tc/Zr ratios untenable.

The theory of the "mini *s*-process" can be tested further by looking at the abundances of elements which can be produced by reaction chains similar to those that produce Tc. The best example is Co which is produced by the reaction ^{58}Ni$(n, \gamma)^{59}$Ni$(\beta\nu)$ ^{59}Co. The half-life of ^{59}Ni is 8×10^4 yr, so in

our calculations it has not been allowed to decay. If the ^{59}Ni is allowed to decay to Co, the resulting Co abundance is the sum of the ^{59}Ni and ^{59}Co entries in Table 6 (which are instantaneous, i.e., without β-decay), resulting in an enhancement of 0.4 dex in Co. Therefore, if a substantial amount of Ni is allowed to decay to Co, the Co abundance should be enhanced as a result of the "mini *s*-process." The Co values derived for our small sample of stars show no enhancement. However, because the half-life of ^{59}Ni is less than that of ^{99}Tc (2×10^5 yr), the "mini *s*-process" could produce an enhancement of Tc without an enhancement of Co if the star is observed significantly less than 10^5 yr after the first thermal pulse.

Although it seems we can postulate a scenario which will reproduce the Tc, Nb, Zr, and Co abundances observed in our sample of stars, the need for almost the entire envelope to have been processed in this manner makes the scenario questionable.

Recently, a second mechanism for producing Tc in M stars has been proposed by Malaney (1989) and Lattanzio & Malaney (1989). In this scenario, ^{99}Tc is produced by the photofission of Th and U by 7 MeV gamma rays produced in CNO shell burning. The ^{99}Tc produced in this manner is mixed to the surface from the region of the CNO shell of the AGB star. According to Malaney, $\sim$5% of the Th and U atoms undergoing fission will have ^{99}Tc as end products so the abundance of Tc produced is $N_{\rm Tc} = 0.05\ N_{\rm U,Th}$. If we follow Malaney's assumption that the *r*-processed elements can be enhanced by up to a factor of 4 above solar and make the further assumption that all Th and U atoms in the vicinity of the CNO shell undergo photofission, then the maximum Tc abundance which can be produced before being diluted with the envelope is $\log (N_{\rm Tc}) \approx 0.8$. If one considers realistic dilution factors, this figure is much too low to explain the Tc abundances in our sample of M stars. Therefore, this scenario suffers from the same problem as the "mini *s*-process" in that dilution with unprocessed envelope material brings the Tc abundance to a level substantially below the values observed.

5. CONCLUSIONS

It does not seem at this juncture that the observations and theories have converged to resolve the question of Tc in M stars. The present study seems to question both present theories, the "mini *s*-process" and photofission mechanism although we feel that the "mini *s*-process" is more likely to be correct. However, the question of the variable Nb abundance raises concerns about the validity of the assumption of similar ionization equilibrium even for elements of similar ionization potential. More observational work needs to be conducted to understand the mechanism which causes the systematic shifts in equivalent width with time. In addition, it would be helpful to obtain very high resolution spectra of the Tc I lines in order to verify that blending is being handled correctly in the analysis of Tc abundances from these lines.

This research was supported by a grant from the Kennilworth Fund of the New York Community Trust. The detailed "mini *s*-process" calculations were performed on the Cray XMP-48 at the National Center for Supercomputing Applications and were supported in part by NSF grant AST-900012. The authors wish to thank the staff of DAO for their hospitality especially Les Saddlemyer and Doug Bond who set up the spectrograph and V. V. Smith for many helpful discussions concerning spectral line synthesis. We would also like to thank A. L. Merts and J. Abdallah of the Los Alamos National Laboratory for performing the calculations of the photoionization cross sections of Co I, Nb I, and Tc I.

APPENDIX A

A comparison of our Tc abundances and Tc/Zr ratios with those of Kipper & Kipper (1984) and of Smith (1988) shows very large discrepancies. We display this unfortunate situation in Table 7. We believe that our abundances and ratios are more nearly correct than those of the other two groups for the following reasons.

Kipper & Kipper used spectra of lower resolution than ours and did not include the hyperfine structure of Tc in synthesizing the 4262 and 4297 Å lines. This will lead to substantial errors in the abundances derived in the synthesis. In fact, they accept that their errors may be as large as one dex.

To assist us in comparing results V. V. Smith has kindly provided us with his measurements of the 4238 Å line of Tc I as well as the 4239 and 4240 Å lines of Zr I in two of the three stars in common in our two studies. We compare the equivalent widths used in the two studies in Table 8. All the equivalent widths from Smith's study are larger than ours. Upon comparison, it is apparent that the

TABLE 7

COMPARISON OF WASHINGTON, TEXAS, AND TARTU ABUNDANCES OF T_c

	$\log N_{\rm Tc}$[a]		
Star	Washington	Texas[b]	Tartu[c]
o^1 Ori	0.5	0.1	2.0
T Cep	1.3	...	1.5
W Cyg	1.35	...	1.5
TU CVn	<0.1	...	2.0
RS Cnc	1.3	...	3.0
HR 8062	0.9	−0.4	...

[a] On the basis of $\log N_{\rm H} = 12.0$.
[b] Smith 1988.
[c] Kipper & Kipper 1984.

TABLE 8

COMPARISON OF WASHINGTON AND TEXAS DATA FOR Tc AND Zr IN TWO STARS

	log W/λ							
	4238 (Tc)		4239 (Zr)		4240 (Zr)		log (Zr/Tc)	
STAR	Texas	Washington	Texas	Washington	Texas	Washington	Texas	Washington
o^1 Ori	4.11	4.47	4.33	4.47	4.23	4.33	3.4	2.3
HR 8062	4.20	4.55	4.35	4.64	4.30	4.44	3.0	1.5

equivalent width of the Tc line provided by Smith is greater than our equivalent width by a factor which is larger than the enhancement of Zr I equivalent widths for both stars. Hence it is impossible for their Zr/Tc ratios to be larger than the ratios derived in this study by over an order of magnitude as indicated by a comparison of results. It appears that their synthesis of the 4262 Å line and it neighboring lines must be in correct for reasons that neither Smith nor ourselves can understand at present.

REFERENCES

Ake, T. B. 1977, Ph.D. thesis, Case Western Reserve University
Anders, E., & Grevesse, N. 1989, it Geochim. Cosmochim. Acta, 53, 197
Bao, Z. Y., & Käppeler, F. 1987, Atomic Data Nuc. Data, 36, 411
Beer, H., Käppeler, F., & Arcoragi, J. P. 1989, in Proc. 5th Workshop on Nuclear Astrophysics, ed. W. Hildebrandt & E. Mueller (Max Planck Institut Proceedings), 6
Burbidge, G. R., Burbidge, E. M., Fowler, W. A., & Hoyle, F. 1957, Rev. Mod. Phys., 29, 54
Boesgaard, A. 1970a, ApJ, 161 163
———. 1970b, ApJ, 161, 1003
Boothroyd, A., & Sackmann, I.-J. 1988, ApJ, 328, 632
Bowen, G. H. 1989, in IAU Symp. 106, Evolution of Peculiar Red Giants, ed. H. R. Johnson & B. Zuckerman (Cambridge: Cambridge Univ. Press), 269
Brown, J. A., Johnson, H. R., Alexander, D. R., Cutright, L. C., & Sharp, C. M. 1989, ApJS, 71, 623
Cameron, A. B. W. 1954, Phys. Rev., 93, 932 (1954)
Cowley, C. R., & Downs, P. L. 1980, ApJ, 236, 648
Dominy, J. F., & Wallerstein, G. 1986, ApJ, 310, 371 (DW)
Garstang, R. H. 1981, PASP, 93, 641
Hinkle, K. H., Hall, D. N. B., & Ridgway, S. 1982, ApJ, 252, 697
Hollowell, D. E., & Iben, I., Jr. 1989, in IAU Colloq. 108, Atmospheric Diagnostics of Stellar Evolution, Lecture Notes in Physics, Vol. 305, ed. K. Nomoto (Berlin: Spring-Verlag), 38
Holmes, J. A., Woosley, S. E., Fowler, W. A., & Zimmerman, B. 1976, Atom. Data Nucl. Data 18, 306
Kipper, T., & Kipper, M. A. 1984, Soviet Astr. Letters, 10, 363
Kipper, T., & Wallerstein, G., 1990, PASP, 102, 574
Lambert, D. L. 1989, in IAU Symp. 106, Evolution of Peculiar Red Giants, ed. by H. R. Johnson & B. Zuckerman (Cambridge: Cambridge Univ. Press), 101
Lattanzio, J. 1989, ApJ, 344, L25
Lattanzio, J., & Malaney, R. 1989, ApJ, 347, 989
Little, S., Little-Marenin, I. R., & Hagen-Bauer, W. 1987, AJ, 94, 981 (LLMB)
Malaney, R. 1989, Nature, 337, 718
Merrill, P. W. 1952, ApJ, 116, 21
Neugebauer, G., & Leighton, R. B. 1969, Two-Micron Sky Survey (Washington, DC: National Aeronautics and Space Administration)
Ratynski, W., & Käppeler, F. 1988, Phys. Rev. C., 37, 595
Ridgeway, S. T., Joyce, R. R., White, N. M., & Wing, R. F. 1980, ApJ, 235, 126
Smith, V. V. 1988, in Origin and Distribution of the Elements, ed. G. J. Mathews (Singapore: World Scientific), 535
Smith, V. V., & Lambert, D. L. 1985, ApJ, 294, 326
———. 1986, ApJ, 311, 843 (SL)
———. 1988, ApJ, 333, 219
Takahashi, K., & Yokoi, K. 1987, Atom. Data, Nucl. Data 36, 375
Wallerstein, G. 1985, PASP, 97, 994
Wallerstein. G., & Dominy, J. F. 1988, ApJ, 330, 937 (WD)
Woosley, S. E., Fowler, W. A., Holmes, J. A., & Zimmerman, B. 1978, Atom. Data Nucl. Data 22, 371
Zook, A. C. 1985, ApJ, 289, 356